ACS OMEGA

Open Access

http://pubs.acs.org/journal/acsodf

Article

Elucidation of the Catalytic Pathway for the Direct Conversion of Furfuryl Alcohol into γ-Valerolactone over Al_2O_3−SiO_2 Catalysts

Pichaya Chuangpusri, Sasiradee Jantasee, Patcharaporn Weerachawanasak, Weerachon Tolek, Chawalit Ngamcharussrivichai, Duangamol N. Tungasmita, Noppadon Sathitsuksanoh, and Joongjai Panpranot*

Cite This: *ACS Omega* 2023, 8, 46560−46568

Read Online

ACCESS | Metrics & More | Article Recommendations | Supporting Information

ABSTRACT: The one-pot conversion of furfuryl alcohol (FA) into GVL was investigated over the sol−gel-synthesized Al_2O_3−SiO_2 (AlSi) catalysts with various Al_2O_3 loadings (0.2−10 wt %) and commercial zeolites including MFI-1, H-ZSM5, H-beta, and HY-15 in a batch reactor under mild reaction conditions (130 °C, 1 bar N_2, and 15−120 min). The reaction pathways depend largely on the acid properties of the catalysts, especially the types of Bronsted (B) and Lewis (L) acid sites. A tandem alcoholysis/hydrogenation/cyclization sequence is dominant on the AlSi catalysts (Al ≥ 4%) and all the zeolites except MFI-1, resulting in complete conversion of FA and GVL with an yield 64−75% with IPL as the major side-product, regardless of the differences in their B/L ratios 0.06−1.35. In the absence of B acid sites (i.e., 0.2% AlSi and MFI-1 catalysts), FA could be straightforwardly converted into GVL on the weak Lewis acid sites from the isolated silanol groups using 2-propanol as a hydrogen source. The AlSi catalysts are promising tunable catalysts for FA conversion with good recyclability.

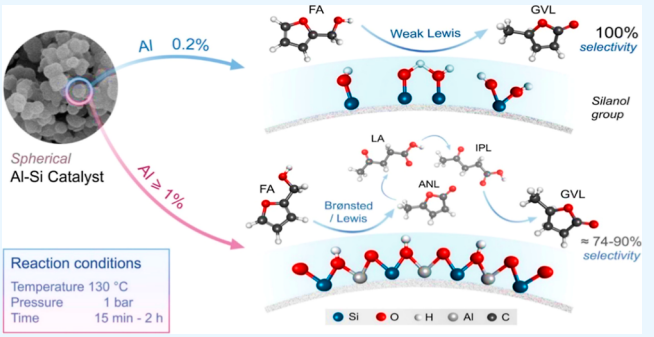

INTRODUCTION

Lignocellulosic biomass is an abundant resource of organic carbon for the production of a variety of industrial chemicals.[1] Xylose, the main sugar produced from hemicellulose hydrolysis, is typically converted into furfural, which is used as a starting raw material for many functionalized molecules such as furan, tetrahydrofurfuran, tetrahydrofurfuryl alcohol, and furfuryl alcohol (FA). Approximately 80% of furfural is converted into FA via catalytic hydrogenation and is utilized in furan resin polymerization.[2] However, higher-value products can be further obtained via hydrolysis of FA to form levulinic acid (LA) and subsequent LA dehydration to produce α-angelica lactone (AnL). Finally, AnL hydrogenation can transform FA to γ-valerolactone (GVL).[3,4] LA is an important building block chemical exploited as a precursor in a variety of applications, including pharmaceuticals, solvent, fuel additive, and flavoring agent.[5] AnL, the high-value biochemical products produced during the conversion process, is applied in the synthesis of natural products, polymers, and biofuels or used as a flavor and cigarette additive. GVL can be used as a solvent, fuel additive, and in the production of perfumes and food additives.[6] One-pot conversion of xylose and furfural into GVL[7] or conversion of LA into GVL[8] has been reported. Due to the similar market price of furfural and FA, it is interesting to use FA as the starting reagent for the production of higher value products such as GVL and AnL.

In a number of studies,[3,7,9,10] strong acid catalysts have been employed in the FA conversion reaction and the major products are lactones, furfuryl ether, and alkyl levulinate, not GVL. Reaction pathways and mechanisms appeared to depend on the type of catalyst used. For example, in the reaction starting with FA in 2-propanol at 130 °C and 1 h reaction time, H-beta produced AnL as the main product, whereas H-ZSM-5 converted FA into iso-propyl furfuryl ether.[9] On the other hand, arene-sulfonic acid-functionalized SBA-15 was reported to be the most efficient catalyst for the production of iso-propyl levulinate from FA in 2-propanol. A few studies including more recent ones reported the production of GVL as one of the major products (% yield GVL 30−94%) from FA using sulfonic acid functionalized ILs and metal catalysts[3] and mesoporous materials Al-SBA-15 functionalized Al/Zr and Au (or Ru) metal.[10] The catalyst synthesis is quite complicated and more costly due to the use of an ionic liquid and noble metal. The multiple steps of conversion of FA into GVL require acidic

Received: July 25, 2023
Revised: November 14, 2023
Accepted: November 15, 2023
Published: December 1, 2023

https://doi.org/10.1021/acsomega.3c05412
ACS Omega 2023, 8, 46560−46568

properties of catalysts including both Lewis acid sites (L) and BrØnsted acid sites (B).[7]

Alumina-silica is an amorphous catalyst with lower acidity than zeolite but is known to be a versatile catalyst being used in several catalytic reactions such as hydrogenation of acrolein,[11] liquid phase alkylation of aromatics, or used as the support for metal, metal oxide, and sulfide catalysts.[12] In a previous study by Chada et al.,[13] $Al_2O_3-SiO_2$ with 10 wt % Al_2O_3 was found to exhibit the highest conversion of FA to alkyl levulinate among the various silica supported metal oxides including $Al_2O_3-SiO_2$, ZrO_2-SiO_2, WO_3-SiO_2, and TiO_2-SiO_2 at 180 °C. The performances of the catalysts were correlated to the presence of a greater number of weak Lewis acidic sites.

In this study, the one-pot conversion of FA into GVL using the metal-free $Al_2O_3-SiO_2$ catalysts synthesized via a facile sol−gel method was carried out and compared to the various commercially available zeolite catalysts such as H-ZSM-5, H-beta, HY, and MFI-1 zeolites under relatively mild reaction conditions of low temperature (130 °C), low pressure, and short reaction time (15−120 min). The catalyst performances were correlated with their physicochemical properties, especially the presence of Lewis and BrØnsted acid sites.

MATERIALS AND METHODS

Materials. FA (98%), α-AnL (98%), GVL (99%), LA (98%), hexadecyltrimethylammonium bromide (CTAB, ≥98%), aluminum nitrate nonahydrate (≥98%), and tetraethyl orthosilicate (TEOS, reagent grade 98%) were purchased form Sigma-Aldrich. Merck supplied ethanol and 2-propanol. Ammonium solution (28%) was obtained from the Quality Reagent Chemical Product (QREC Asia). All reagents were used as received without further purification.

Preparation of $Al_2O_3-SiO_2$ Catalysts. The $Al_2O_3-SiO_2$ (AlSi) catalysts were synthesized by the sol−gel technique using CTAB (3.35 g) as a structure directing agent. CTAB was dissolved at room temperature inside a solution of ethanol (80.16 g), deionized (DI) water (64.71 g), and an ammonium solution (18.7 g) stirred at 350 rpm. Then, to generate the gel composition, TEOS as a silica precursor and aluminum nitrate nonahydrate as an alumina precursor were slowly doped into the solution and mixed for 2 h. The gel solution was then filtered and rinsed with DI water until the pH reached 7. Finally, the solids were dried overnight at 110 °C and calcined in air at 650 °C for 6 h at a heating rate of 2 °C/min. These catalysts were labeled as *x* % AlSi, where *x* is the percentage of Al_2O_3 loading by weight.

Commercial Zeolites. All commercial zeolites were purchased from supplier. HY zeolites was purchased from Sasol, NH_4-ZSM-5 was purchased from Riogen Catalysis for Chemicals & Energy, and NH_4−beta and silicalite-1 (MFI-1) were purchased from TOSOH Corperation Co., Ltd. The NH_4ZSM5 and NH_4beta catalysts were calcined in air under similar conditions of preparation of *x*% AlSi catalysts to form H-ZSM5 and H-beta.

Catalyst Characterization. X-ray diffraction (XRD) studies were performed on a Bruker AXS model D8 Discover with Cu of the X-ray tube in the range of 1−10° for mesoporous *x*% AlSi catalysts and determined with Cu K_α radiation from 20 to 50° for commercial zeolites. X-ray fluorescence (XRF) spectrometry with a BRUKER S8 TIGER is a technique for determining the actual amounts of alumina and silica in the catalyst. Surface area, pore volume, and mean pore diameters were quantified using the N_2 physisorption technique in a Micrometrics ASAP 2020 instrument with the Brunauer−Emmett−Tellet (BET), Barrett−Joyner−Halenda, and the 4 V_p/S_{BET} equation. The sample was outgassed under vacuum before being analyzed at −196 °C. The solid-state spectra were recorded using Fourier transform nuclear magnetic resonance (NMR) spectrometer technique at 400 MHz with a BRUKER AVANCE III HD/Ascend 400 WB. Meanwhile, adamantane was employed as a reference standard in ^{1}H MAS NMR, aluminum chloride hexa-hydrate ($AlCl_3 \cdot 6H_2O$) was used as a reference in ^{27}Al MAS NMR, and sodium trimethylsilypropanesulfonate (DSS) was used as a reference in ^{29}Si MAS NMR. The resonance frequency of 400.2 MHz was used to record the ^{1}H, ^{27}Al, and ^{29}Si MAS NMR spectra. The chemical environment of H, Al, and Si of the catalysts was revealed by the NMR spectra. The total acidity of the catalysts was measured by the temperature-programmed desorption of ammonia (NH_3-TPD) using a Micromeritics ChemiSorb 2750 with ChemiSoftTPx software. The quartz *U*-tube was filled with 0.1 g of fresh catalyst. The adsorbed water and organic matters were eliminated by pretreating the catalyst in helium at 600 °C, afterward absorbing the sample at ambient temperature with 3 vol % NH_3/He (25 mL/min) on the acid sites. The catalyst was purged with pure He at a rate of 25 mL/min until a constant baseline was achieved and then heated to 550 °C at a rate of 10 °C/min. It was held in this state for an hour. The temperature at which NH_3 is absorbed on the acid sites correlates with the catalyst's acid strength. A criterion for the acid sites classification is described as the desorption temperature of 100−150, 150−250, and 250−500 °C defined for weak, medium, and strong acid sites, respectively.[14−16] In order to examine a number of Lewis and BrØnsted acidic sites on the catalysts, in situ pyridine FTIR spectroscopy (Py-FTIR) was conducted in a NICOLET iS10 FTIR spectrometer (Thermo Fisher Scientific, Waltham, MA, USA). The sample was placed in a quartz cell equipped with CaF_2 windows after it became pressed on a self-supporting disc. The sample disc was then pretreated at 550 °C for 1 h under vacuum to remove certain impurities. The operating temperature was again lowered to 50 °C. Pyridine vapor was injected into the cell until the adsorption reached equilibrium, next the cell was evacuated for 15 min at the same temperature. The spectra were recorded for a total of 96 scans. The corresponding bands were deconvoluted for better assignment using OriginPro 8.5 software version 85E (OriginLab Corporation, Northampton, MA, USA). The contents of both BrØnsted and Lewis acidic sites were quantified using an extinction coefficients.

One-Pot Conversion of FA and Calculation of Products. FA was converted into valuable biochemical products in a batch autoclave reactor with a capacity of 100 mL. In the autoclave, 1.15 mmol FA was dissolved in 20 mL of 2-propanol in the autoclave reactor. The catalytic test was then carried out by placing 0.12 g of catalyst in the autoclave. The autoclave was heated to 130 °C after being pressurized with 1 bar of N_2. To start the reaction, the stirrer was turned on at 800 rpm after the temperature reached its target point. The reaction was kept at this condition for 15 or 120 min. The catalyst was centrifuged out of the solution once the temperature was brought to room temperature. After that, the liquid product was analyzed by gas chromatography with a flame ionization detector (GC−FID) and RTX-5 capillary column. The calculation of the substance, high-value products, and carbon balance were based on the area below peak at retention time of the chemicals detected from GC−FID.

https://doi.org/10.1021/acsomega.3c05412
ACS Omega 2023, 8, 46560−46568

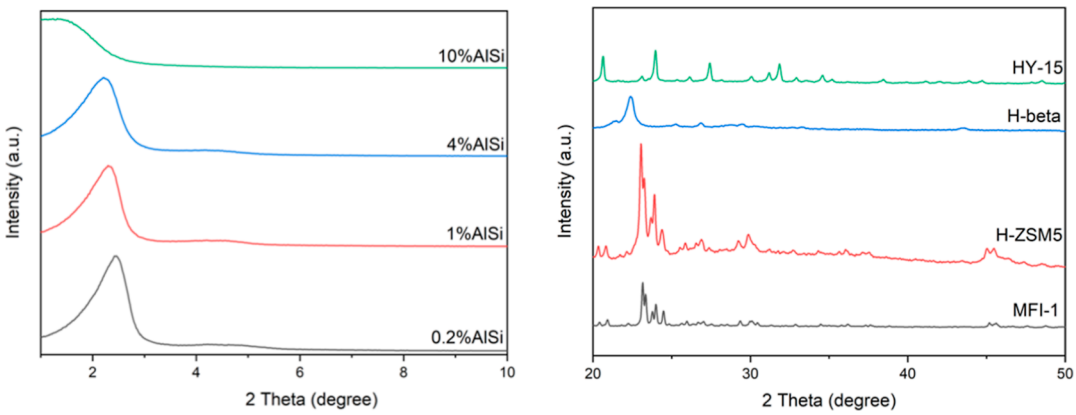

Figure 1. XRD patterns of the mesoporous *x*% AlSi (left) and commercial zeolite (right) catalysts.

$$\text{Conversion}(\%) = \left[\frac{\text{area of FA initial} - \text{area of FA final}}{\text{area of FA initial}}\right] \times 100$$

$$\text{Selectivity}i(\%) = \left[\frac{\text{area of product}i}{\text{total area of all products}}\right] \times 100$$

Conversion = the conversion of FA. Selectivity *i* = the selectivity of product *i*, where *i* represents AnL, GVL, and IPL.

RESULTS AND DISCUSSION

Characteristics of the Catalysts. Figure 1 shows the powder XRD pattern analysis of *x*% AlSi catalysts in low angles.[17] The diffraction peaks ~2.2−2.5° and 4.1−4.5° 2 theta correspond to (100) and (110) planes within a hexagonal structure,[18−20] which are typical for an ordered mesoporous silica. The (110) diffraction peak disappeared for 10% Al loading.[21] The crystallinity of the commercial zeolite catalysts was confirmed by obvious XRD patterns.

The Si/Al ratios of the AlSi catalysts containing 0.2−10 wt % Al were in the range of 5.2−294.0 as determined from the XRF results (Table 1). The Si/Al ratio of 4% AlSi (Si/Al = 13.1) was comparable to those of H-ZSM5, H-beta, and HY-15 zeolites (Si/Al ratios 11.4−14.0). The specific surface area (S_{BET}), pore volume (V_p), and mean pore diameter were determined by N_2 adsorption−desorption techniques, respectively, and the results are presented in Table 1. The S_{BET} and V_p of the AlSi catalysts decreased with increasing Al_2O_3 loading from 1071 to 435 m^2/g and 0.89 to 0.52 cm^3/g, respectively, while the mean pore diameters were slightly increased from 2.1 to 3.7 nm. The nitrogen sorption isotherms of the AlSi catalysts indicate a type IV isotherm in the IUPAC classification (Figure 2.). 0.2% AlSi, 1% AlSi, 4% AlSi, and MFI-1 showed type H1 hysteresis loop corresponding to a narrow range of uniform mesoporous structures, which is in accordance with the XRD results, whereas 10% AlSi, H-ZSM5, H-beta, and HY-15 zeolite exhibited type H3 hysteresis loop, which was attributed to the meso-/macropore network (in addition to their micropores).[22] For a similar Si/Al ratio, the 4% AlSi had a larger specific surface area and pore volume (mesopores) than H-ZSM5, H-beta, and HY-15. The scanning electron microscopy (SEM) images of the AlSi and zeolite catalysts are shown in Figures S1−S2, respectively. All the AlSi catalysts exhibited a uniform spherical shape with a smooth surface with particle sizes ranging from 300 nm to 1 μm. The H-ZSM5, H-beta, and HY-15 catalysts are irregularly shaped. The MFI-1 catalyst has a small mean diameter of around 150 nm.

Table 1. XRF and N_2 Physisorption Results of the Catalysts

catalysts	Si/Al ratio[a]	S_{BET} (m^2/g)	pore volume (V_p) (cm^3/g)	mean pore diameter (nm)
0.2% AlSi	294.0	1071	0.89	2.1
1% AlSi	63.8	977	0.87	2.1
4% AlSi	13.1	949	0.87	2.3
10% AlSi	5.2	435	0.52	3.7
MFI-1		386	0.28	7.7
H-ZSM5	11.5	328	0.17	8.3
H-beta	14.0	580	0.34	4.6
HY-15	11.4	514	0.17	10.8

[a]Si/Al ratio were determined by XRF.

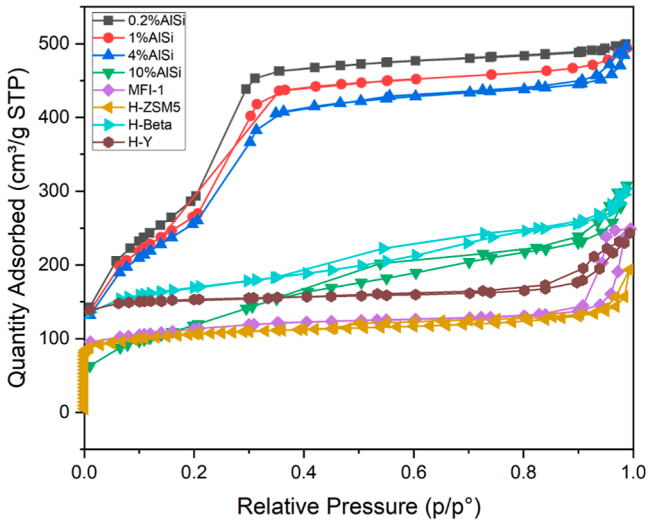

Figure 2. N_2 adsorption−desorption isotherms of AlSi and commercial zeolite catalysts.

Table 2 presents the surface acidity of x%AlSi and commercial zeolite catalysts based on the NH_3-TPD results. Supporting Information Figure S3 depicts the NH_3-TPD profiles of all catalysts. The area below the ammonia desorption peaks provides information on the total amount of surface acidity, while the peak position in the temperature ranges 100−150, 150−200, and 250−500 °C is defined as weak, medium, and strong acid strength, respectively.[14] The AlSi catalysts with

https://doi.org/10.1021/acsomega.3c05412
ACS Omega 2023, 8, 46560−46568

Table 2. Acidity of the Catalysts and Amount of Brønsted Acid and Lewis Acid Sites

catalysts	weak acidity[a]	medium acidity[a]	strong acidity[a]	total surface acidity[a]	Brønsted acid[b] (B)	Lewis acid[b] (L)	B + L[b]	ratio B/L[b]
0.2% AlSi	165.4			165.4		0.23	0.23	
1% AlSi	254.1			254.1		0.12	0.12	
4% AlSi	160.7	96.7		257.5	0.03	0.47	0.49	0.06
10% AlSi	138.4	96.2	294.9	529.4	0.11	0.36	0.47	0.31
MFI-1	198.7	53.9		252.5		0.42	0.42	
H-ZSM5	196.1	889.0	645.5	1730.6	0.68	0.51	1.19	1.35
H-beta	410.1	335.9	732.4	1478.4	0.47	0.57	1.04	0.82
HY-15	67.0	86.6	336.9	490.5	0.30	0.66	0.96	0.45

[a]Acidity of catalysts (μmol/g) were determined by NH_3-TPD. [b]Amount B, L, B + L acid sited (mmol/g catalysts) and ratio B/L were determined by in situ py-IR at 100 °C.

relatively low Al_2O_3 contents such as 0.2% AlSi and 1% AlSi and the MFI-1 catalyst, which has no Al_2O_3 in the framework, showed only weak acid sites.[23,24] The total surface acidity and acid strength of the AlSi catalysts increased with an increasing Al_2O_3 content. The 4% AlSi contained only weak and medium acid sites. Strong acid sites were additionally found in the 10% AlSi. All the commercial zeolites, including H-ZSM5, H-beta, and HY-15 had higher amount of strong acid sites than the AlSi catalysts, especially H-ZSM5 and H-beta, in which their acidities were double those of AlSi.

The in situ pyridine-IR spectra indicating Brønsted and Lewis acid sites in these catalysts and stability of acidic sites in the temperature range 50−400 °C are displayed in Figure 3. The acid strength is defined from which pyridine is removed by evacuation at 100−200 and 200−400 °C as medium acid strength and strong acid strength, respectively.[25] The amounts of Brønsted and Lewis acid sites are listed in Table 2. The bands in the pyridine-IR spectra at approximately 1445 and 1455 cm^{-1} were assigned to the Lewis acid sites (L). The peak at 1577 cm^{-1} was attributed to the high silica containing weak Lewis (WL), mainly from abundant silanol nest.[26] Hydrogen-bound pyridine (H) at 1595 cm^{-1} indicates the hydrogen bond interaction between pyridine and the surface of the catalysts. Al is indeed a good strong Lewis acid Al (SL), which can be identified by the IR peak centered at 1623 cm^{-1}.[25−28] The peak positions for SL, L, and B were clearly detected for the catalysts with a substantial quantity of Al_2O_3. However, for the 0.2% AlSi and MFI-1 catalysts that contained high silica loading exhibited only WL and L acid sites. Besides, all the peaks disappeared at temperature greater than 150 °C, suggesting that they were weak acid sites. The in situ pyridine-IR results are in good agreement with the NH_3-TPD results.

The ^{1}H MAS NMR, ^{27}Al MAS NMR, and ^{29}Si MAS NMR results of the AlSi catalysts are displayed in Figure 4. In the ^{1}H MAS NMR spectra, the peaks at 1.8 and 2.1 ppm were assigned to isolated silanol groups at the SiO_2 surface and the signals in the range of 2.2−2.7 ppm are assigned to low acidic −OH groups to nonframework aluminum species (AlOH).[29,30] These peaks were detected on low Al loading (0.2−4 wt %) AlSi. The peak at 3−3.5 ppm represents the structures involving with the silanol groups and physisorbed water on the silica surface.[31] For 4% AlSi, the broad peak at 3.7 due to a range of bridging hydroxyl groups attached to more than one aluminum ion and/or to those between Si and Al atoms is apparent. Moreover, the peak at 3.7−4.2 ppm range found on 4% AlSi and 10% AlSi indicates the Brønsted acid site.[30,32]

Al atoms in the catalysts were characterized by ^{27}Al MAS NMR. The spectra of x% AlSi catalysts present two peaks around 54 and 0 ppm, which can be referred to as Al^{IV} tetrahedrally coordinated and Al^{VI} octahedrally coordinated, respectively. The big peak of Al^{IV} suggests that most of Al species are coordinated in the mesoporous framework.[21] The intensity of both Al^{IV} and Al^{VI} peaks increased with the increasing Al content.[33] Moreover, the peak at 34 ppm indicates the Al^{V} site, which interacts with local SiOH groups to generate Brønsted acid sites.[34] ^{29}Si MAS NMR has become a standard method to structurally characterize the silicates. The spectra of all AlSi catalysts show broadened signals in the −89, −98, and −108 ppm. The peaks around −89, often referred to as Q_2 silicons or as geminal silanol, which is attributed to silicon atoms that have two hydroxyl groups attached, $(SiO)_2Si(OH)_2$. The resonance around −98 ppm is ascribed to silicon with the only one hydroxyl group $(SiO)_3Si(OH)_3$, and is referred to as Q_3 silicons, i.e., vicinal or isolated silanols. The signal around −108 ppm indicates Q_4 silicons or surfaces siloxanes $Si(OSi)_4$, are in the neighborhood of silanol groups which are not chemically bonded to any hydroxyl group.[35−38]

Catalytic Performances in One-Pot Conversion of FA. The catalytic performances of x% AlSi and commercial zeolite catalysts in the one-pot conversion of FA to GVL are shown in Table 3. A control experiment without the catalyst showed around 6.4% FA conversion at 130 °C and 120 min. We suggested that FA conversion is a thermal conversion because FA converted into IPL and GVL. We synthesized AlSi catalysts by the sol−gel method and varied the percent weight of alumina loading to contribute to the FA conversion to valuable products. The 0.2% AlSi catalyst increased the FA conversion from 7.7 to 22% and was directly selective to GVL (100%). Likewise, the alumina content was increased from 0.2% Al to 1% Al which raised FA conversion up to 84.5%. We observed that 0.2% AlSi had the lowest total acidity, and almost all acidity presented a weak Lewis acid site (WL). The lowest alumina loading on silica (0.2% AlSi) could not activate another acidity, only WL acid sites were indicated from the silanol group on the silica surface, as also confirmed by the pyridine-IR results (Figure 3.). On the other hand, AlSi catalysts, with larger amount of alumina loading (≥1%) did not provide 100% GVL selectivity. The performance of commercial zeolite without Al in the framework (MFI-1) was investigated along with the other commercially available zeolites, including H-ZSM5, H-beta, and HY-15 for the conversion of FA to valuable chemical products at 130 °C for 120 min. Interestingly, we observed the performance of MFI-1 as similar to that of 0.2% AlSi catalyst, which suggested that the WL acid site was the main acid site for the FA conversion to GVL with 100% selectivity. Meanwhile, H-ZSM5 exhibited the highest GVL selectivity at around 77%. It is interesting that H-ZSM5 possessed a larger B/L ratio than 4% AlSi but they exhibited similar GVL selectivity. It is possible that the B/L

https://doi.org/10.1021/acsomega.3c05412
ACS Omega 2023, 8, 46560−46568

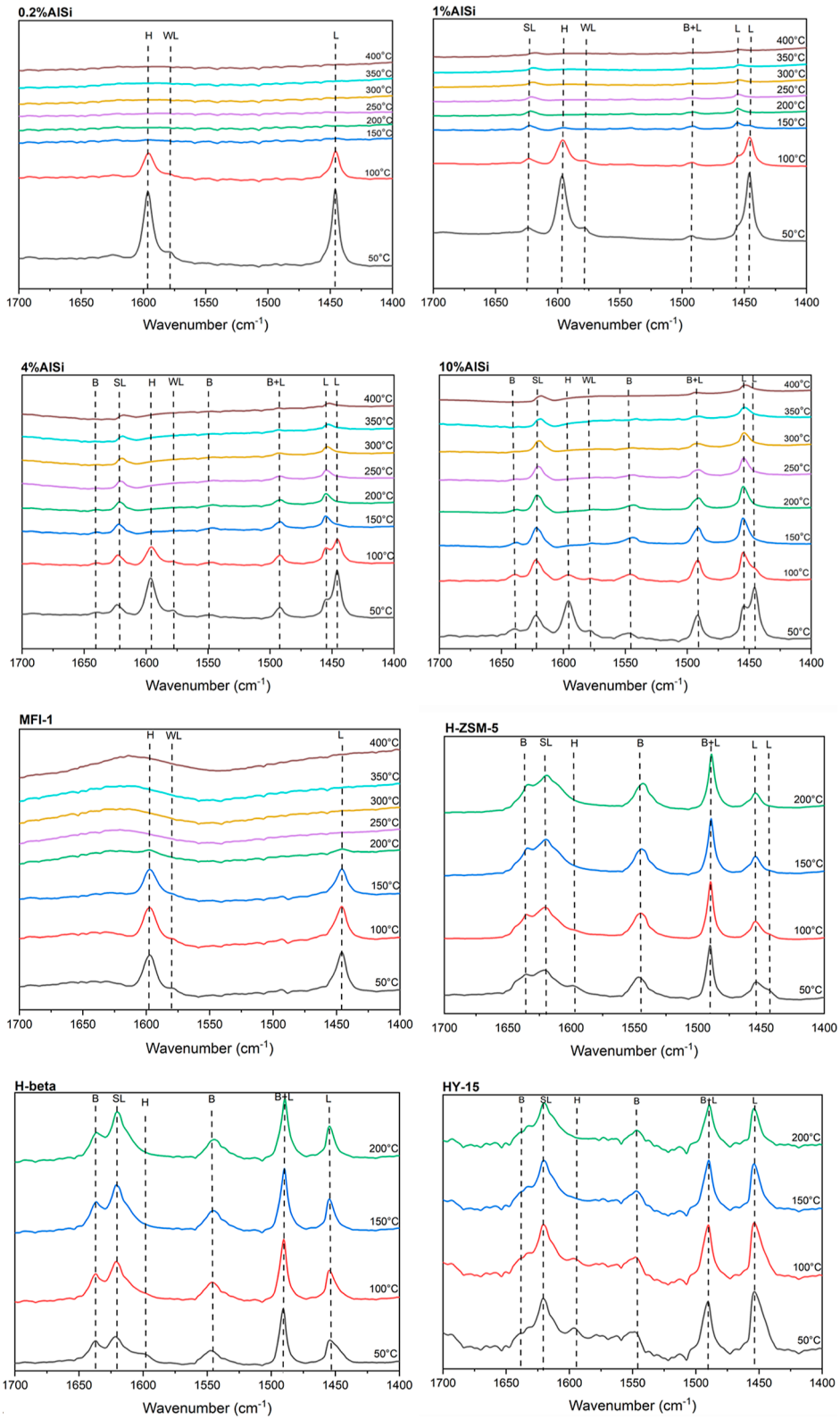

Figure 3. In situ pyridine-IR desorption spectra of 0.2% AlSi, 1% AlSi, 4% AlSi, 10% AlSi, MFI-1, H-ZSM-5, H-beta, and HY-15 samples at the different temperatures, which characteristic bands are for hydrogen-bound pyridine (H), pyridine adsorbed on Brønsted (B), Lewis (L), strong Lewis (SL), and weak Lewis (WL).

ratios in the range 0.06−1.35 did not have much influence on the one-pot conversion of FA into GVL in IPA under the reaction conditions used.

Typically, acidic catalysts and alcohol media, which are hydrogen donors in the reaction, are necessary in the one-pot conversion of FA to GVL. A comparison of FA conversion from various catalytic systems from the previous studies in the

https://doi.org/10.1021/acsomega.3c05412
ACS Omega 2023, 8, 46560−46568

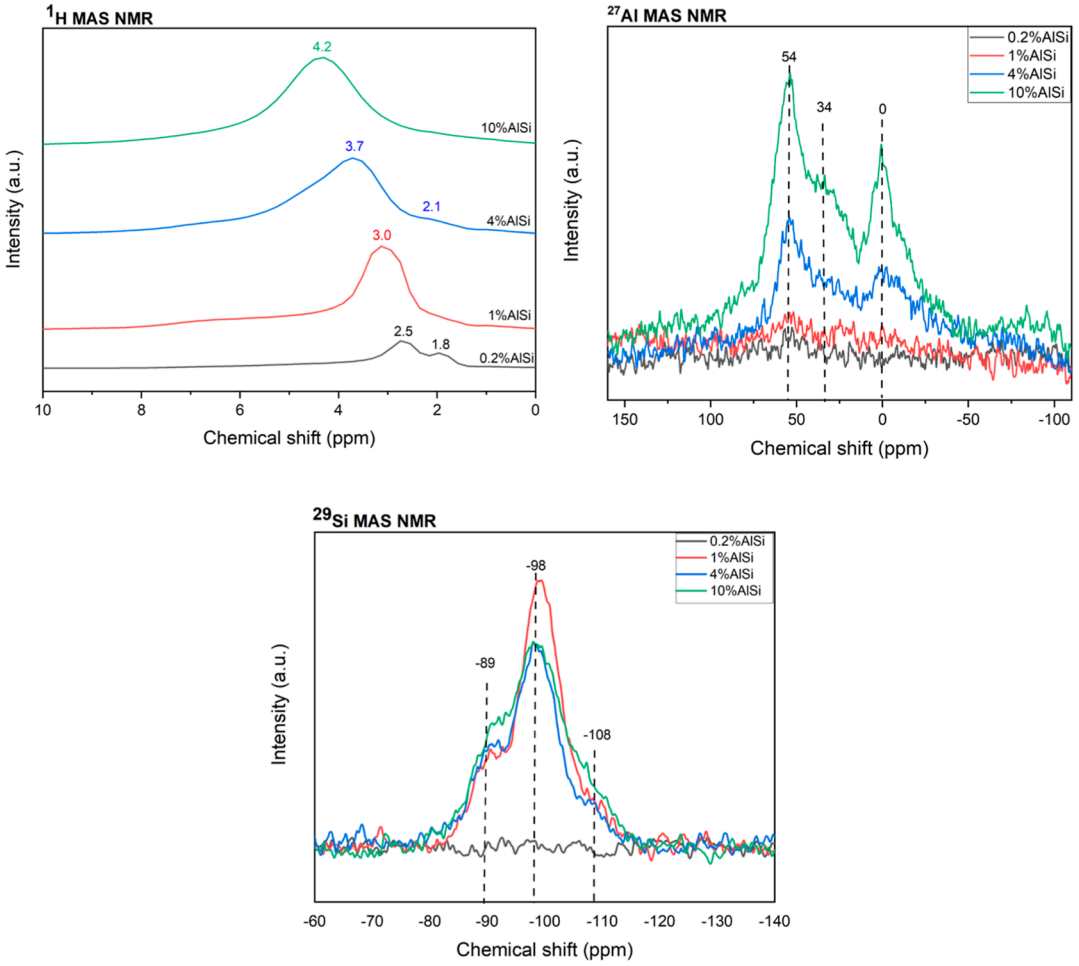

Figure 4. ^{1}H, ^{27}Al, and ^{29}Si MAS NMR spectra of 0.2% AlSi, 1% AlSi, 4% AlSi, and 10% AlSi catalysts.

Table 3. Catalytic Performances of the Catalysts for FA Conversion into GVL[a]

			selectivity (%)			
catalysts	reaction time (min)	conversion (%)	AnL	GVL	IPL	others (%)
blank	120	6.4	0	46.1	28.9	25.0
0.2% AlSi	120	22.0	0	100	0	0
1% AlSi	120	84.5	0.8	82.5	15.3	1.4
4% AlSi	120	100	1.0	73.2	24.6	1.2
10% AlSi	120	100	1.3	75.2	22.3	1.3
MFI-1	120	18.4	0	100	0	0
H-ZSM5	15	30.9[b]	0.4	98.5	1.2	0
	120	100	0	76.6	23.4	0
H-beta	120	100	3.6	67.3	22.2	6.9
HY-15	120	99.7	1.4	63.5	33.4	1.7

[a]Reaction conditions: FA 100 μL, 2-propanol 20 mL, catalyst weight 0.12 g, temperature 130 °C, stirred 800 rpm, N_2 1 bar, reaction time 120 min. [b]Catalyst weight 0.018 g, for 15 min. Error of measurements ±5%.

literature is shown in Table S1. It has been reported that the one-pot conversion of FA to GVL with 94% yield was obtained using sulfonic acid functionalized ILs in combination with 10% Ru/C catalysts.[3] High amounts of metal sites are necessary for hydrogenation of methyl levulinate to GVL in the tandem reactions of alcoholysis and hydrogenation of methyl levulinate. Over the γ-Fe_2O_3/HZSM-5, relatively high GVL yield >90% was optimized at 130 °C in 2-propanol at 8 h reaction time.[39] According to Shao et al., loading of Cu metal can increase GVL production on H-ZSM5.[40] The selective synthesis of GVL from FA occurs via a tandem alcoholysis/hydrogenation/cyclization sequence. From the previous studies, both L and B acid sites are involved in the multistep reaction from FA to GVL. In agreement with these previous studies, all the commercial zeolites and the AlSi catalysts that contain both L and B acid sites yielded relatively high GVL selectivity (>60%) and complete conversion of FA in IPA with HZSM-5 and 10% AlSi exhibiting the highest GVL yield ~75−77% in 2 h reaction time at 130 °C. It has been suggested by Bendeddouche et al.[41] that increasing the alumina content in sol−gel-derived AlSi catalysts can increase the conversion of lignocellulosic biomass into valuable bioproducts. Complete FA conversion could be achieved after 2 h of reaction time with our AlSi catalysts with alumina loading ≥4%. The conversion of FA was still more than 90% for 15 min reaction time with GVL selectivity ~80% (Table S2). It should be noted that the pure silica catalyst prepared by the sol−gel method exhibited 26.6% FA conversion with a GVL selectivity of 73.6% in 60 min of reaction time. Nevertheless, other byproducts were produced at around 26.4% on the pure silica, whereas the MFI-1 catalyst gave 100% selectivity toward GVL without any byproducts.

Among the various zeolites, the formation of AnL was slightly higher on the H-beta zeolite. Such results agree well with the results in the literature that beta zeolite provides lactones as the

https://doi.org/10.1021/acsomega.3c05412
ACS Omega 2023, 8, 46560−46568

main product probably due to the diffusional limitation of FA-derived intermediates in the microporous structure of beta zeolite that favors AnL formation,[9,42] which can be produced directly from FA without FE intermediates.[9] HY-15 with the largest three-dimensional pore network with interconnected pores could minimize the mass transfer limitation, leading to higher IPL selectivity.[9] In this study, IPL was also found to be the major side product. Typically, on B acid sites, IPL can directly be obtained from alcoholysis of FA by IPA and then L acid sites are necessary to facilitate the MPV reaction to produce (alkyl) 4-hydroxy pentanoic acid intermediates, which are further lactonized into the GVL product.[39,43−45] For the catalysts containing only WL acid sites (0.2% AlSi and MFI-1 catalysts), it was found that only GVL was formed with 100% selectivity despite their low FA conversion. It is proposed that FA can be straightforwardly converted into GVL on the WL acid site from the isolated silanol groups using 2-propanol as a hydrogen source. The reaction network starting from FA to valuable bioproducts is shown in Figure 5. The different acid

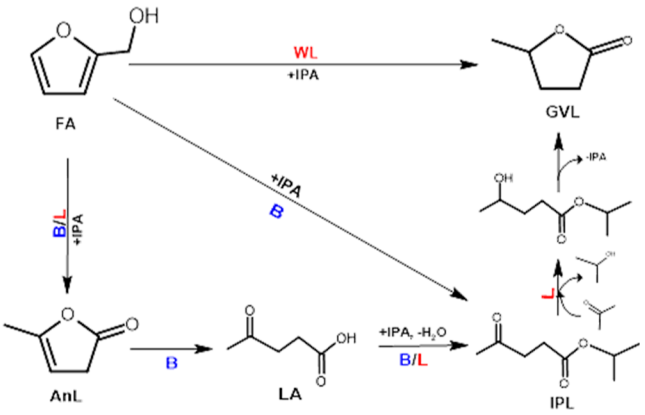

Figure 5. Proposed reaction network for the conversion of FA into GVL.

properties, including L, SL, WL, and B acid sites, can alter the reaction pathways in the one-pot conversion of FA into GVL over the SiAl and zeolite catalysts.

Catalyst Reusability. The 4% AlSi catalyst shows advantages in the reusability in the conversion of FA to GVL. The reusability of the catalyst was tested for four cycles at 130 °C and 15 min in the batch autoclave reactor. After completion of each cycle, the catalyst was recovered by centrifugation, washed with 2-propanol, dried in an oven overnight, and calcined in air at 650 °C for 6 h before being reused in the next run. The conversion of FA and products selectivity are shown in Figure 6. The conversions of FA in all runs are not different, at around 98% conversion. The GVL selectivity slightly decreased from 78% in the first batch to around 72% for the reused catalysts. The results confirmed that the AlSi catalyst is a flexible catalyst with good reusability.

CONCLUSIONS

The one-pot conversion of FA into GVL in 2-propanol at 130 °C for 120 min was carried out using Al_2O_3−SiO_2 catalysts with various Al_2O_3 loadings (0.2−10% AlSi) prepared by the sol−gel method and compared with commercial zeolites (MFI-1, H-ZSM5, H-beta, and HY-15) under the same reaction. FA conversion and GVL selectivity were found to be dependent on acidity types and catalyst structures under the reaction

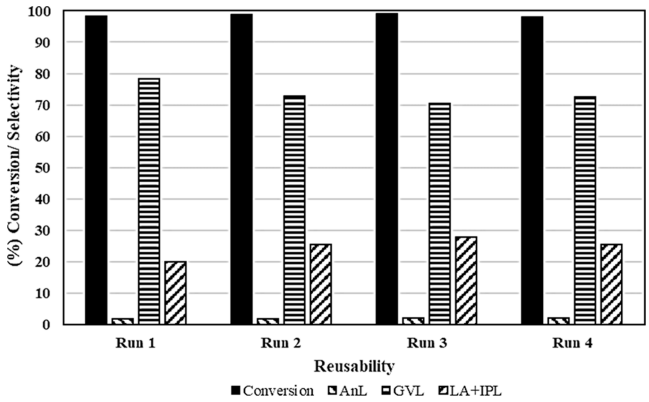

Figure 6. Recycle study of 4% AlSi in the conversion of FA to GVL. Reaction conditions: FA 100 μL, 2-propanol 20 mL, catalyst weight 0.12 g, temperature 130 °C, stirred 800 rpm, N_2 1 bar, and reaction time 15 min.

conditions used (reaction temperature 130 °C and reaction time 15−120 min in an alcohol media). Weak Lewis acid sites from silanol groups (i.e., 0.2% AlSi and MFI-1) can directly convert FA with 100% GVL selectivity but with relatively low conversion. Meanwhile, BrØnsted acid sites can increase FA conversion up to 100% but it decreased GVL selectivity and produced other biochemicals such as AnL and IPL. All the Al_2O_3−SiO_2 catalysts with Al loading ≥1 wt % showed good performances comparable to the commercial zeolites and exhibited good reusability in four consecutive runs without activity loss.

ASSOCIATED CONTENT

Supporting Information

The Supporting Information is available free of charge at https://pubs.acs.org/doi/10.1021/acsomega.3c05412.

Comparison of FA conversion from various catalytic systems, catalytic performances for 15 min, and catalysts characterization by SEM and NH_3-TPD (PDF)

AUTHOR INFORMATION

Corresponding Author

Joongjai Panpranot − *Center of Excellence on Catalysis and Catalytic Reaction Engineering, Department of Chemical Engineering, Faculty of Engineering, Chulalongkorn University, Bangkok 10330, Thailand; Bio-Circular-Green-economy Technology & Engineering Center, BCGeTEC, Department of Chemical Engineering, Faculty of Engineering, Chulalongkorn University, Bangkok 10330, Thailand;* orcid.org/0000-0002-0398-5912; Email: joongjai.p@chula.ac.th

Authors

Pichaya Chuangpusri − *Center of Excellence on Catalysis and Catalytic Reaction Engineering, Department of Chemical Engineering, Faculty of Engineering, Chulalongkorn University, Bangkok 10330, Thailand*

Sasiradee Jantasee − *Department of Chemical and Materials Engineering, Faculty of Engineering, Rajamangala University of Technology Thanyaburi, Pathum, Thani 12110, Thailand*

Patcharaporn Weerachawanasak − *Industrial Chemistry, Department of Chemistry, Faculty of Science, King Mongkut's Institute of Technology Ladkrabang, Bangkok 10520, Thailand*

https://doi.org/10.1021/acsomega.3c05412
ACS Omega 2023, 8, 46560−46568

Weerachon Tolek − *Center of Excellence on Catalysis and Catalytic Reaction Engineering, Department of Chemical Engineering, Faculty of Engineering, Chulalongkorn University, Bangkok 10330, Thailand*

Chawalit Ngamcharussrivichai − *Department of Chemical Technology, Faculty of Science, Chulalongkorn University, Bangkok 10330, Thailand;* orcid.org/0000-0002-5621-8880

Duangamol N. Tungasmita − *Department of Chemistry, Faculty of Science, Chulalongkorn University, Bangkok 10330, Thailand*

Noppadon Sathitsuksanoh − *Department of Chemical Engineering, University of Louisville, Louisville, Kentucky 40292, United States*

Complete contact information is available at: https://pubs.acs.org/10.1021/acsomega.3c05412

Notes

The authors declare no competing financial interest.

■ ACKNOWLEDGMENTS

The Second Century Fund of Chulalongkorn scholarship for P.C. and financial supports from the National Research Council of Thailand (NRCT)—Research Team Promotion grant (Joongjai Panpranot) and the Thailand Science Research and Innovation (TSRI) through Program Management Unit for Competitiveness (PMU-C) (contract number C10F640006) are gratefully acknowledged.

■ REFERENCES

(1) Shinde, S. H.; Hengne, A.; Rode, C. V. *Biomass, Biofuels, Biochemicals*; Elsevier, 2020, pp 1−31.
(2) Zeitsch, K. J. *Sugar series*; Elsevier, 2000; Vol. *13*.
(3) Hengne, A. M.; Kamble, S. B.; Rode, C. V. Single pot conversion of furfuryl alcohol to levulinic esters and γ-valerolactone in the presence of sulfonic acid functionalized ILs and metal catalysts. *Green Chem.* **2013**, *15*, 2540−2547.
(4) Lima, C. G. S.; Monteiro, J. L.; de Melo Lima, T.; Paixão, M. W.; Corrêa, A. G. Angelica Lactones: From Biomass-Derived Platform Chemicals to Value-Added Products. *ChemSusChem* **2018**, *11*, 25−47.
(5) Wang, H.; Yang, B.; Zhang, Q.; Zhu, W. Catalytic routes for the conversion of lignocellulosic biomass to aviation fuel range hydrocarbons. *Renew. Sustain. Energy Rev.* **2020**, *120*, 109612.
(6) Climent, M. J.; Corma, A.; Iborra, S. Conversion of biomass platform molecules into fuel additives and liquid hydrocarbon fuels. *Green Chem.* **2014**, *16*, 516−547.
(7) Coelho, T. L.; Marinho, B.; Albuquerque, E. M.; Fraga, M. A. Discussing the performance of beta zeolites in aqueous-phase valorization of xylose. *Catal. Sci. Technol.* **2020**, *10*, 7165−7176.
(8) Koley, P.; Rao, B. S.; Shit, S. C.; Sabri, Y.; Mondal, J.; Tardio, J.; Lingaiah, N. One-pot conversion of levulinic acid into gamma-valerolactone over a stable Ru tungstosphosphoric acid catalyst. *Fuel* **2021**, *289*, 119900.
(9) Paniagua, M.; Melero, J.; Iglesias, J.; Morales, G.; Hernández, B.; López-Aguado, C. Catalytic upgrading of furfuryl alcohol to bio-products: Catalysts screening and kinetic analysis. *Appl. Catal., A* **2017**, *537*, 74−82.
(10) Lázaro, N.; Ronda-Leal, M.; Pineda, A.; Osman, S. M.; Shokouhimehr, M.; Jang, H. W.; Luque, R. One-pot multi-step synthesis of gamma-valerolactone from furfuryl alcohol: Microwave vs continuous flow reaction studies. *Fuel* **2023**, *334*, 126439.
(11) Volckmar, C. E.; Bron, M.; Bentrup, U.; Martin, A.; Claus, P. Influence of the support composition on the hydrogenation of acrolein over Ag/SiO2-Al2O3 catalysts. *J. Catal.* **2009**, *261*, 1−8.
(12) Busca, G. Silica-alumina catalytic materials: A critical review. *Catal. Today* **2020**, *357*, 621−629.
(13) Chada, R. R.; Koppadi, K. S.; Enumula, S. S.; Kondeboina, M.; Kamaraju, S. R. R.; Burri, D. R. Continuous Synthesis of Fuel Additives Alkyl Levulinates via Alcoholysis of Furfuryl Alcohol over Silica Supported Metal Oxides. *Catal. Lett.* **2018**, *148*, 1731−1738.
(14) Adnan, M. A.; Muraza, O.; Razzak, S. A.; Hossain, M. M.; de Lasa, H. I. Iron oxide over silica-doped alumina catalyst for catalytic steam reforming of toluene as a surrogate tar biomass species. *Energy Fuels* **2017**, *31*, 7471−7481.
(15) Hongrutai, N.; et al. Differences in acid and catalytic properties of W incorporated spherical SiO2 and 1% Al-doped SiO2 in propene metathesis. *Catal. Today* **2020**, *424*, 112964.
(16) Nie, R.; Lei, H.; Pan, S.; Wang, L.; Fei, J.; Hou, Z. Core-shell structured CuO-ZnO@H-ZSM-5 catalysts for CO hydrogenation to dimethyl ether. *Fuel* **2012**, *96*, 419−425.
(17) Zhang, Z.; Han, Y.; Zhu, L.; Wang, R.; Yu, Y.; Qiu, S.; Zhao, D.; Xiao, F. S. Strongly acidic and high-temperature hydrothermally stable mesoporous aluminosilicates with ordered hexagonal structure. *Angew. Chem., Int. Ed.* **2001**, *40*, 1258−1262.
(18) Gusev, V. Y.; Feng, X.; Bu, Z.; Haller, G. L.; O'Brien, J. A. Mechanical stability of pure silica mesoporous MCM-41 by nitrogen adsorption and small-angle X-ray diffraction measurements. *J. Phys. Chem.* **1996**, *100*, 1985−1988.
(19) Soares, D. C. F.; de Sousa Andrada, A.; Ramaldes, G. A. Silica nanoparticles containing gadolinium complex as potential alternative to anticancer radiotherapy. *Part. Sci. Technol.* **2015**, *33*, 331−338.
(20) Das, S.; Manam, J.; Sharma, S. K. Role of rhodamine-B dye encapsulated mesoporous SiO2 in color tuning of SrAl2O4: Eu2+, Dy3+ composite long lasting phosphor. *J. Mater. Sci.: Mater. Electron.* **2016**, *27*, 13217−13228.
(21) Li, Y.; Yang, Q.; Yang, J.; Li, C. Synthesis of mesoporous aluminosilicates with low Si/Al ratios using a single-source molecular precursor under acidic conditions. *J. Porous Mater.* **2006**, *13*, 187−193.
(22) Thommes, M.; Kaneko, K.; Neimark, A. V.; Olivier, J. P.; Rodriguez-Reinoso, F.; Rouquerol, J.; Sing, K. S. Physisorption of gases, with special reference to the evaluation of surface area and pore size distribution (IUPAC Technical Report). *Pure Appl. Chem.* **2015**, *87*, 1051−1069.
(23) Wang, W.; Zhou, W.; Li, W.; Xiong, X.; Wang, Y.; Cheng, K.; Kang, J.; Zhang, Q.; Wang, Y. In-situ confinement of ultrasmall palladium nanoparticles in silicalite-1 for methane combustion with excellent activity and hydrothermal stability. *Appl. Catal. B Environ.* **2020**, *276*, 119142.
(24) Weng, M.; Zhang, Z.; Okejiri, F.; Yan, Y.; Lu, Y.; Tian, J.; Lu, X.; Yao, S.; Fu, J. Encapsulation of CuO nanoparticles within silicalite-1 as a regenerative catalyst for transfer hydrogenation of furfural. *Iscience* **2021**, *24*, 102884.
(25) Li, X.; Peng, K.; Liu, X.; Xia, Q.; Wang, Y. Comprehensive Understanding of the Role of Brønsted and Lewis Acid Sites in Glucose Conversion into 5-Hydromethylfurfural. *ChemCatChem* **2017**, *9*, 2739−2746.
(26) Yi, F.; Chen, Y.; Tao, Z.; Hu, C.; Yi, X.; Zheng, A.; Wen, X.; Yun, Y.; Yang, Y.; Li, Y. Origin of weak Lewis acids on silanol nests in dealuminated zeolite Beta. *J. Catal.* **2019**, *380*, 204−214.
(27) Zhao, X.; Wen, T.; Zhang, J.; Ye, J.; Ma, Z.; Yuan, H.; Ye, X.; Wang, Y. Fe-Doped SnO2 catalysts with both BA and LA sites: facile preparation and biomass carbohydrates conversion to methyl lactate MLA. *RSC Adv.* **2017**, *7*, 21678−21685.
(28) Zhang, W.; Wang, P.; Yang, C.; Li, C. A Comparative study of n-butane isomerization over H-Beta and H-ZSM-5 zeolites at low temperatures: effects of acid properties and pore structures. *Catal. Lett.* **2019**, *149*, 1017−1025.
(29) Gabrienko, A. A.; Danilova, I. G.; Arzumanov, S. S.; Toktarev, A. V.; Freude, D.; Stepanov, A. G. Strong acidity of silanol groups of zeolite beta: Evidence from the studies by IR spectroscopy of adsorbed CO and 1H MAS NMR. *Microporous Mesoporous Mater.* **2010**, *131*, 210−216.
(30) Hensen, E. J. M.; Poduval, D. G.; Degirmenci, V.; Ligthart, D. J. M.; Chen, W.; Maugé, F.; Rigutto, M. S.; Veen, J. R. v. Acidity

characterization of amorphous silica-alumina. *J. Phys. Chem. C* **2012**, *116*, 21416−21429.
(31) Protsak, I. S.; Morozov, Y. M.; Dong, W.; Le, Z.; Zhang, D.; Henderson, I. M. A 29Si, 1H, and 13C solid-state NMR study on the surface species of various depolymerized organosiloxanes at silica surface. *Nanoscale Res. Lett.* **2019**, *14*, 160−215.
(32) Müller, M.; Harvey, G.; Prins, R. Comparison of the dealumination of zeolites beta, mordenite, ZSM-5 and ferrierite by thermal treatment, leaching with oxalic acid and treatment with SiCl4 by 1H, 29Si and 27Al MAS NMR. *Microporous Mesoporous Mater.* **2000**, *34*, 135−147.
(33) Valla, M.; Rossini, A. J.; Caillot, M.; Chizallet, C.; Raybaud, P.; Digne, M.; Chaumonnot, A.; Lesage, A.; Emsley, L.; van Bokhoven, J. A.; et al. Atomic description of the interface between silica and alumina in aluminosilicates through dynamic nuclear polarization surface-enhanced NMR spectroscopy and first-principles calculations. *J. Am. Chem. Soc.* **2015**, *137*, 10710−10719.
(34) Zhao, Y.; Wang, L.; Kochubei, A.; Yang, W.; Xu, H.; Luo, Y.; Baiker, A.; Huang, J.; Wang, Z.; Jiang, Y. Formation and Location of Pt Single Sites Induced by Pentacoordinated Al Species on Amorphous Silica-Alumina. *J. Phys. Chem. Lett.* **2021**, *12*, 2536−2546.
(35) Liu, C. C.; Maciel, G. E. The fumed silica surface: A study by NMR. *J. Am. Chem. Soc.* **1996**, *118*, 5103−5119.
(36) Qu, L.; Zhang, W.; Kooyman, P. J.; Prins, R. MAS NMR, TPR, and TEM studies of the interaction of NiMo with alumina and silica-alumina supports. *J. Catal.* **2003**, *215*, 7−13.
(37) Aerts, A.; Follens, L. R. A.; Haouas, M.; Caremans, T. P.; Delsuc, M. A.; Loppinet, B.; Vermant, J.; Goderis, B.; Taulelle, F.; Martens, J. A.; et al. Combined NMR, SAXS, and DLS study of concentrated clear solutions used in silicalite-1 zeolite synthesis. *Chem. Mater.* **2007**, *19*, 3448−3454.
(38) Del Rosal, I.; Gerber, I. C.; Poteau, R.; Maron, L. Grafting of lanthanide complexes on silica surfaces dehydroxylated at 200 °C: a theoretical investigation. *New J. Chem.* **2015**, *39*, 7703−7715.
(39) Lima, T. M.; Lima, C. G. S.; Rathi, A. K.; Gawande, M. B.; Tucek, J.; Urquieta-González, E. A.; Zbořil, R.; Paixão, M. W.; Varma, R. S. Magnetic ZSM-5 zeolite: a selective catalyst for the valorization of furfuryl alcohol to γ-valerolactone, alkyl levulinates or levulinic acid. *Green Chem.* **2016**, *18*, 5586−5593.
(40) Shao, Y.; Li, Q.; Dong, X.; Wang, J.; Sun, K.; Zhang, L.; Zhang, S.; Xu, L.; Yuan, X.; Hu, X. Cooperation between hydrogenation and acidic sites in Cu-based catalyst for selective conversion of furfural to γ-valerolactone. *Fuel* **2021**, *293*, 120457.
(41) Bendeddouche, W.; Bedrane, S.; Zitouni, A.; Bachir, R. Highly efficient catalytic one-pot biofuel production from lignocellulosic biomass derivatives. *Int. J. Energy Res.* **2021**, *45*, 2148−2159.
(42) Antunes, M. M.; Lima, S.; Neves, P.; Magalhães, A. L.; Fazio, E.; Fernandes, A.; Neri, F.; Silva, C. M.; Rocha, S. M.; Ribeiro, M. F.; et al. One-pot conversion of furfural to useful bio-products in the presence of a Sn,Al-containing zeolite beta catalyst prepared via post-synthesis routes. *J. Catal.* **2015**, *329*, 522−537.
(43) Bui, L.; Luo, H.; Gunther, W. R.; Roman-Leshkov, Y. Domino Reaction Catalyzed by Zeolites with Brønsted and Lewis Acid Sites for the Production of γ-Valerolactone from Furfural. *Angew. Chem., Int. Ed. Engl.* **2013**, *52*, 8022−8025.
(44) Antunes, M. M.; Lima, S.; Neves, P.; Magalhães, A. L.; Fazio, E.; Neri, F.; Pereira, M. T.; Silva, A. F.; Silva, C. M.; Rocha, S. M.; et al. Integrated reduction and acid-catalysed conversion of furfural in alcohol medium using Zr, Al-containing ordered micro/mesoporous silicates. *Appl. Catal. B Environ.* **2016**, *182*, 485−503.
(45) Luo, Y.; Yi, J.; Tong, D.; Hu, C. Production of γ-valerolactone via selective catalytic conversion of hemicellulose in pubescens without addition of external hydrogen. *Green Chem.* **2016**, *18*, 848−857.

https://doi.org/10.1021/acsomega.3c05412
ACS Omega 2023, 8, 46560−46568